JOURNAL OF OPTOELECTRONICS AND ADVANCED MATERIALS Vol. 19, No. 5 - 6, May – June 2017, p. 412 - 416

Structural, morphological and electrical properties of Zn doped PbS thin films by chemical spray pyrolysis technique

M. G. FARAJ*, F. A. I. CHAQMAQCHEE, H. D. OMAR
Department of Physics, Faculty of Science and Health, Koya University, University Park, Danielle Mitterrand Boulevard, Koya KOY45, Kurdistan Region-F.R. Iraq

In this work, structural and electrical properties of Zinc doped lead sulfide (PbS) thin films are benign reported. Lead sulfide thin films with different Zn doping concentrations (0, 1, 2, and 3 at %) were deposited on glass substrates using the chemical spray pyrolysis technique. Effect of Zn doping on the structural, morphological and electrical properties of the films was studied. The X-ray diffraction (XRD) studies revealed that all the films exhibit face centered cubic structure with a preferred orientation along the (2 0 0) plane irrespective of Zn doping concentration. Thus, the film′s grains decreased in size with increasing Zn content. Scanning tunneling microscopy (STM) measurements is showed that the surface roughness of the films is decreased due to zinc doping as well. In addition, X-ray fluorescence (XRF) was used for elemental analysis of films regarding Zn concentrations. The accuracy is determined by comparing the XRF data with 1, 2 and 3 at-% Zn dopants concentrations. Finally, electrical studies revealed that the film coated with 3 at-% Zn dopant has a maximum carrier concentration of 1.39×10^{10} cm^{-3}. The obtained results infer that the (PbS: Zn) film coated with 3 at% Zn dopant has better structural, morphological and electrical properties.

(Received June 23, 2016; accepted June 7, 2017)

Keywords: Zn doping effects, PbS, Thin films, Structural properties, Electrical properties

1. Introduction

In recent studies, II-IV and IV-VI semiconductors materials has been the subject of great interest due to their applications in the field of optoelectronics, infrared sensors, solar coating, gas humidity sensors and photo electrochemical solar cells [1-3]. In addition, IV-VI semiconductors compound such as PbS has a cubic lattice with unit cell face center cube. These semiconductor materials have important properties as direct band gap and narrow gap with band gap energy of 0.4 eV [4-6].

PbS has wide spectrum applications, which includes gas sensors, bio sensors, infrared detectors, solar radiation selective absorber coating, solar radiation control coating, decorative coating and field effect transistors [7-11]. Chemical spray pyrolysis, chemical bath deposition, successive ionic layer adsorption and reaction (SILAR) and thermal evaporation techniques have been reported for the deposition of PbS thin films [12-15].

In the present work, the effect of zinc incorporation on the properties of PbS thin films is reported. The films were fabricated using chemical spray pyrolysis techniques. The effect of Zn doping on the structural, morphological and electrical properties of the films was investigated. Accommodation of wide range of Zn into the PbS lattice can improve its electrical properties.

2. Experimental details

The undoped PbS and the Zn-doped PbS (PbS: Zn) thin films were deposited by chemical spray pyrolysis technique. Chemicals that used for the deposition of PbS and PbS:Zn films were lead (II) acetate trihydrate ($Pb(CH_3CO_2)_2\cdot3H_2O$, Thiourea ($CS(NH_2)_2$) and zinc acetate $Zn(CH_3COO)_2$. All the chemicals were of analytical reagent grade (sigma make, with a purity of 99.9%).

The PbS films were prepared by mixing aqueous solutions of lead (II) acetate trihydrate ($Pb(CH_3CO_2)_2\cdot3H_2O$ and Thiourea ($CS(NH_2)_2$), molarities of 0.1 M and appropriate volumes with a distilled water. This is done by using magnetic stirrer for 30 minutes and the resultant solution was sprayed on glass substrates using chemical spray pyrolysis technique at 300°C. Zinc acetate with different concentrations of 0, 1, 2 and 3 at % were added to start solution for zinc doping. The thicknesses of the Zn-doped PbS thin films were of the order of 400 nm, measured with an optical reflectometer (Model: Filmetrics F20). X-ray diffraction data of undoped and Zn-doped PbS thin films was determined with a high resolution of X-ray diffractometer system (Model: Panalytical Empyrean) with CuKα radiation (λ=1.5406 Å) X-ray source. Surface morphological studies were also carried out using a Scanning Tunneling Microscope (STM) (Model: NT-MDT Solver Nano). Furthermore, the compositions of the films were estimated with Energy Dispersive X-ray Fluorescence Spectrometer (Model: Rigaku-NEX CG).

Finally, the electrical properties of thin films were measured by Hall measurements (HL5500PC) system.

3. Results and discussion

3.1. Structural properties

XRD patterns of PbS:Zn thin films using various Zn concentrations (0,1, 2, and 3 at%) are shown in Fig.1. The presence of more than one peak indicates that PbS:Zn thin films are polycrystalline. It show that XRD patterns for all films have sharp peaks of (1 1 1) and (2 0 0) planes along with minor peaks of (2 2 0), (3 1 1) and (2 2 2) planes of cubic crystal structure. This result corresponded to pure PbS (JCPDS Card no. 05-0592) with a preferred orientation along the (200) plane. It is evident from XRD spectra, that there are no additional peaks for the doped ones when compared to the PbS, which indicates the incorporation of Zn ion into the Pb lattice [16].

The crystalline grain size (t) of the films was determined using Scherrer formula [17].

$$t = \frac{0.9\lambda}{\beta cos\theta} \quad (1)$$

where β is the full width at half maximum (FWHM) of the peak, λ is the wavelength of the X-ray of 1.5406 Å , and θ is their peak position. Based upon the line width of the (200) diffraction peak, the crystallite size is found to be in the range between 41.88 to 14.73 nm for (x = 0- 3 at %).

For the undoped PbS film (Zn content of zero), the crystallites sizes was found to be around 41.88 nm, while for the other films, the crystallites sizes decreased ranging from 30.87 to 14.73 nm with increasing Zn content, as shown in Fig. 2. This behavior approximates with previous reports [18-21].

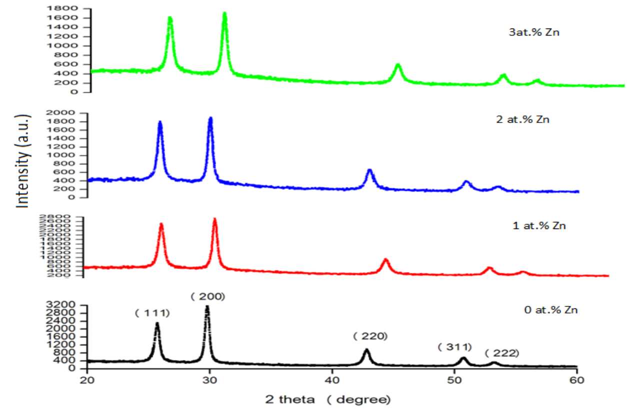

Fig.1. XRD patterns of PbS:Zn thin films with Zn concentrations of 0, 1, 2, and 3 at%

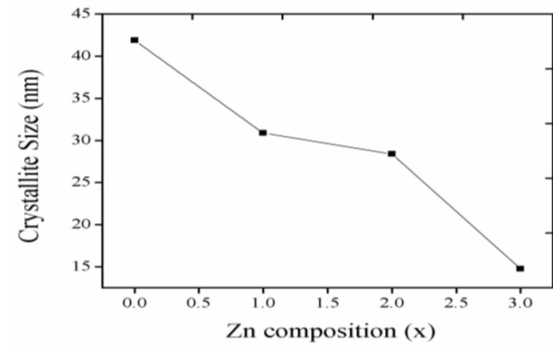

Fig. 2. Crystallites sizes as a function of Zn content is measured

The micro-strain (ε) can be calculated using the formula [22]

$$\varepsilon = \frac{\beta\cos\theta}{4} \quad (2)$$

The values of inter-planar spacing (d) and lattice constant (a) for the cubic phase structure are calculated by reported formulas [23].

$$d_{hkl} = \frac{a}{\sqrt{h^2 + k^2 + l^2}} \quad (3)$$

Table 1. The 2θ values, inter-planar spacing, lattice parameter and micro strain of Zn:PbS thin films as a function of Zn content are shown

Zn content (at%)	2θ value (^{0})	Inter-planner (d) A^0	Lattice constant A^0	Micro Strain (ε)
0	30.1015	2.9973	5.9946	0.00523646
1	30.0424	2.9885	5.977	0.00480776
2	29.8984	2.9745	5.949	0.00357848
3	29.8089	2.9688	5.9376	0.00178828

The inter-planer spacing and their lattice constant are decreased with increasing doping concentration as shown in Table 1. The decrease in the lattice constant is attributed to the incorporation of Zn ions into the Pb lattice sites. It may be due to smaller ionic radius of Zn ion (0.74 Å) compared with Pb ion (1.19Å) as previously reported [16, 20].

It is clear that, the micro strain decreases with increasing the doping concentration. This type of change in strain is due to the predominant re-crystallization

process in the polycrystalline thin films, which agrees with earlier reported results [24].

STM images for surface morphologies of PbS and PbS:Zn thin films are shown in Fig. 3. The value of the root mean square (rms) is the most widely used parameter to characterize the surface roughness. The rms roughness of the pure PbS and (1-3 at %) Zn-doped PbS thin films were found to be around 21.3 to 10.27 nm, respectively. The STM results reveal that the surface roughness decreases with increasing Zn concentrations. This result is agrees with previously reported results [25].

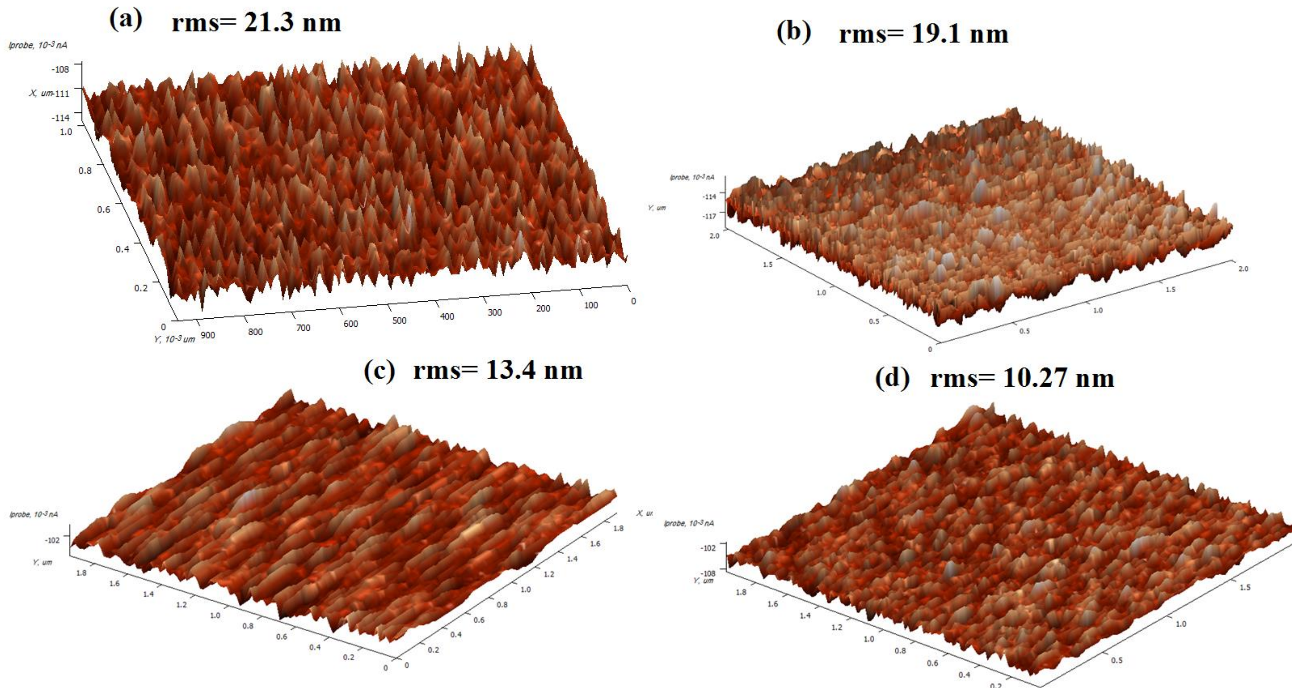

Fig.3. STM analysis of films with (a) undoped PbS, (b) Zn (1 at %), (c) Zn (2 at %) and (d) Zn (3 at %)

Furthermore, XRF analyses were used to confirm the elements of PbS:Zn thin films, where Zn has different concentrations of 1, 2, and 3 at%. When the films are irradiated with X-rays, the intensity as a function of energy can be calculated over the energy range 0-12 KeV at the same computing conditions. Fig. 4 shows the peaks in the ranges of 1.01, 2.30, 2.34 and 10.55 KeV corresponding to Zn-L_α, S-k_α, Pb-M_α and Pb-L_α lines. Note that the Pb-L_α for the film with concentration of 1 at% has the highest peak intensity than the other films of 2 and 3 at%, while the Zn with 1, 2 and 3 at% have the lowest peak intensity due to the doping contents.

As for the quantitative results, Fig. 5 displays mass concentrations (given in mg of the element per m^2 of vacuum pumped) for several representative elements (Pb, Si, S and Zn) of three films, while the inset of figure depicts the masses of the investigated films with various Z contents. It can be seen that, the results are in good agreement, in spite of mass elements had statistical errors with values less than 1%, which is a reasonable in this work. The presence of Si peak in Fig. 4 is due to the glass substrate.

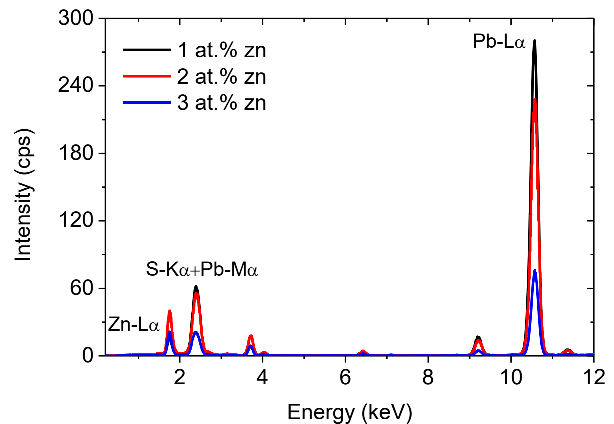

Fig. 4. XRF spectra are measured for the thin films at the same emitted conditions using various Zn contents

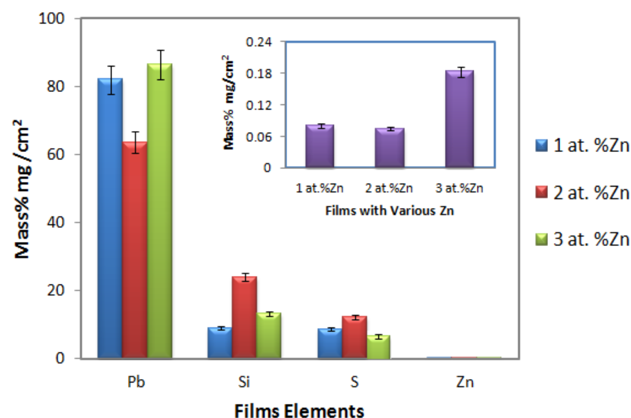

Fig. 5. Comparation of concentration of selected elements of Pb, Si, S and Zn in the same Zn contents of 1, 2 and 3 at % films that measured by XRF. Inset of the figure shows masses of the films as a function of various Zn contents

3.2. Electrical Properties

The dependence of the electrical resistivity and the carrier concentration on the Zn content of PbS thin film are shown in Table 2. The results indicate that PbS films with different Zn ratios are always exhibit p-type conductivity.

The resistivity of the all films decrease with increasing Zn concentrations is due to increase carrier concentration and because of substitutional incorporation of Zn ions in the PbS structure. The reduction of the resistivity can be also attributed to the rise of carriers due to sulfur deficiencies [18,26].

Table 2. Dependence of electrical resistivity and carrier on the Zn content of the films

Zn content (at %)	Resistivity (Ω.m)	Carrier concentration (cm^3)	Conduction type
0	$2.1x10^3$	$0.63 x10^{10}$	P
1	$1.3x10^3$	$0.85x10^{10}$	P
2	$0.93x10^3$	$1.1x10^{10}$	P
3	$0.76x10^3$	$1.39x10^{10}$	P

4. Conclusions

PbS:Zn thin films with different Zn concentrations were fabricated on glass substrates by chemical spray pyrolysis technique. XRD data showed the polycrystalline nature of the film and that it's crystal orientation peak intensities decreased with higher doping concentration of Zn. The crystallite size of the films decreases from 30.87 to 14.73 nm with increase in the zinc composition (x). STM measurements revealed that the surface roughness of the films is decreased due to zinc doping as well. XRF is also used to confirm the accuracy of data with 1, 2 and 3 at-% Zn dopants, where the elements Pb, Si, S, and Zn found in different concentrations. Finally, Hall effect measurements show that Zn doping has an obvious influence on the carrier concentration and resistivity of the PbS thin films. The carrier concentration increases from 0.63×10^{10} cm^3 up to 1.39×10^{10} cm^3 as the Zn concentration increases from 0 to 3 at%. The lowest electrical resistivity of $0.76 x10^3 \Omega$ cm is obtained at 3 at% Zn doping.

Acknowledgements

Hereby we would like to thank my home university "Koya University" and my sponsor the Ministry of Higher Education (MHE) of Kurdistan Regional Government (KRG) for enabling this study.

References

[1] J. Y. Yu, H. Shengshui, Thin Solid Films **516**, 6048 (2008).
[2] A. S. Obaid, M. A. Mahdi, Z. Hassan, M. Bououdina, Materials Science in Semiconductor Processing **15**, 564 (2012).
[3] P. K. Nair, M. T. S. Nair, Semiconductor Science and Technology **4**, 807 (1989).
[4] X. Zhang, M. Lu, International Journal of Infrared and Millimeter Waves **21,** 1697 (2000).
[5] D. Kumara, G. Agarwal, B. Tripathi, D. Vyas, V. Kulshrestha, Journal of Alloys and Compounds **484**, 463 (2009).
[6] S. Seghaier, N. Kamoun, R. Brini, B. A. Amara, Materials Chemistry and Physics **97**, 710 (2006).
[7] F. Tiexiang, Sensors and Actuators B **140**, 116 (2009).
[8] S. Xiaofang, L. Zhaoxia, C. Yan, P. Yuehong, International Journal of Electrochemical Science **6**, 3525 (2011).
[9] H. Hiroshi, H. Kenji, Bulletin of the Chemical Society of Japan **44**, 2420 (1971).
[10] H. W. Jamie, H. Norman, R.-D. Halina, Materials Letters **60**, 3332 (2006).
[11] B. K. Gupta, R. Thangaraj, O. P. Agnihotri, Solar Energy Materials **1,** 481 (1979).
[12] L. Raniero, C. L. Ferreira, L. R. Cruz, A. L. Pinto, R. M. P. Alves, Physica B: Condensed Matter **405**, 1283 (2010).

[13] M. Sharon, K.S Ramaiah, M. Kumar, M. Neumann-Spallart, C. Levy, Journal of Electroanalytical Chemistry **436**, 49 (1997).
[14] B. Thangaraju, P. Kaliannan, Semiconductor Science and Technology **15**, 849 (2000).
[15] J. Puiso, S. Tamulevicius, S. Lindroos, M. Leskela, V. Snitka, Thin Solid Films **428**, 223 (2003).
[16] R. Yousefi, M. Cheragizade, F. Jamali-Sheinic, R. M. Mahmoudian, A. Saaedi, M. N. Huang, Chin. Phys. **B 23**, 108101 (2014).
[17] L. Birks, Journal of Applied Physics. **17**, 687 (1946).
[18] V. T. Sivaraman, S. V. Nagarethinam, R. A. Balu, Progress in Natural Science: Materials International **25**, 392 (2015).
[19] S. Nasrin, S. Manjura Hoque, F. Chowdhury, M. Moazzam Hossen, IOSR Journal of Applied Physics. **6**, 58 (2014).
[20] R. Niruban Bharathi, S. Sankar, International Journal of ChemTech Research. **7**, 980 (2014).
[21] M. Anbarasi, V.S. Nagarethinam, R. Baskaran, V. Narasimman, Pacific Science Review A: Natural Science and Engineering **18**, 72 (2016).
[22] P. P. Hankare, P. A. Chate, D. J. Sathe, P. A. Chavan, M. Bhuse, Journal of Material Science: Materials in Electronics **20,** 374 (2009).
[23] B. D. Cullity, Elements of X-ray diffraction. Addison-Wilson Publishing Company Inc, 42 (1959).
[24] F. A. Kroger, The chemistry of imperfect crystal North-Holland, Amsterdam (1964).
[25] B. Touati, A. Gassoumi, S. Alfaify, N. Kamoun-Turki, Materials Science in Semiconductor Processing **34,** 82 (2015).
[26] S. Ravishankar, A. R. Balu, Studies on ternary PbZnS films suited for optoelectronic applications. Surface Engineering. In Press, p. 1 (2017)

*Corresponding author: mohammad.ghaffar@koyauniversity.org